Available online at www.sciencedirect.com
SCIENCE DIRECT®
ELSEVIER
Sensors and Actuators A 114 (2004) 460–465
SENSORS AND ACTUATORS A PHYSICAL
www.elsevier.com/locate/sna

Fluid–structure coupling analysis and simulation of a micromachined piezo microjet

Changgeng Liu [a,*], Tianhong Cui [b], Zhaoying Zhou [c], Kun Lian [a], Jost Goettert [a]

[a] *Center for Advanced Microstructures and Devices, Louisiana State University, Baton Rouge, LA 70806, USA*
[b] *Institute for Micromanufacturing, Louisiana Technical University, Ruston, LA 71272, USA*
[c] *Department of Precision Instruments, Tsinghua University, Beijing 100084, China*

Received 24 July 2003; received in revised form 4 November 2003; accepted 12 November 2003

Available online 20 January 2004

Abstract

A piezoelectric microjet has been fabricated and its working mechanism has been investigated. Considering different physical effects, the coupling models of the device are established and the key characteristics of the microjet are simulated by finite-element method. The dynamic displacement responses of the transducer under liquid-loading and unloading are calculated and compared. From numerical results, the coupling interactions dramatically damp the vibration amplitude of the transducer. However, the effects on the resonant frequencies of the structure are negligible, which will save much calculation work during further design optimization of the device. Based on the optimal design rules, the device has been fabricated and characterized.
© 2003 Elsevier B.V. All rights reserved.

Keywords: Micromachining; Microjet; Coupling analysis; Simulation

1. Introduction

As an important non-invasive drug delivery method, the atomizing drug method has become the hot research topic for pharmacy and medical instruments. The new atomizing devices have an enormous potential market in the future [1]. In some biochemical experiments, atomized chemicals were released to an artificial environment to control the ingredients precisely [2]. Aerosol of liquid medicine or chemical samples generated by the existing atomizing methods has a rather broad size distribution of droplets and a low control accuracy of the effective dose of medicine or chemicals, which are the most important characteristics of an aerosol generator.

To solve these problems, recently much attention has been drawn to micromachining techniques for the development of new atomizing devices [3–6]. Among the known research, a piezoelectrically actuated microjet [5,6], based on the basic principle of drop-on-demand ink-jets, is more likely to be used as an atomizer for liquid medicine. One of the advantages is that the size of droplets generated by this device is well defined by the size of nozzles and the driving frequency. Moreover, owing to the device actuated electrically, the dose of liquid medicine or chemical samples is easily controlled with high accuracy. In addition, the simple structure and batch microfabrication provide the possibility of minimizing the device to a low-cost portable instrument.

Until now, however, research work has mainly focused on experimentation, fabrication and processing. Only few simple analytical [6] and numerical models [7] have been reported. The theoretical and numerical analysis of the coupling of different fields involved in the device is still in its infancy. Based on the experimental results of the micromachined devices, this paper successfully establishes a piezoelectricity–structure coupling model of the bimorph transducer, investigates the mechanism of releasing liquids through small nozzles and studies the coupling interactions of piezoelectricity, fluidics and structures. Finally, by simplifying the fluid-coupling effect as a dynamic load, the displacement response of the transducer is simulated and the optimal design of the transducer has been obtained.

2. Device fabrication

In general, the device consists of a fluid chamber, which is formed by a piezoelectric bimorph transducer bonded to

* Corresponding author. Tel.: +1-225-578-9944; fax: +1-225-578-6954.
E-mail address: cliu3@lsu.edu (C. Liu).

0924-4247/$ – see front matter © 2003 Elsevier B.V. All rights reserved.
doi:10.1016/j.sna.2003.11.019

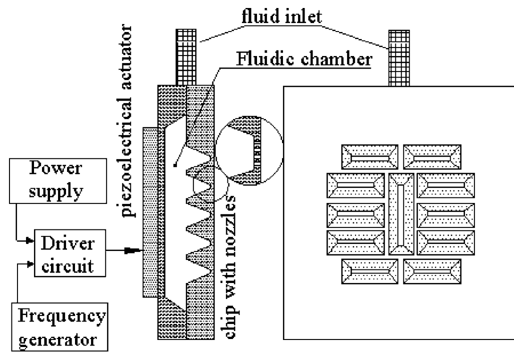

Fig. 1. Structure of a microjet and its driving system.

a silicon chip with nozzle arrays. After optimized by static and dynamic analysis, the nozzle arrays are distributed as shown in Fig. 1.

The silicon chip 3.5 mm × 3.5 mm at the right side of the fluidic chamber is etched by KOH to form 15 μm membrane arrays. By using the inductively coupled plasma (ICP) etching technique, 640 nozzles with the diameter of 5 μm are fabricated through the membrane arrays as shown in Fig. 2. The other silicon chip at the left side of the fluidic chamber is etched by KOH on one side to form an elastic membrane 10 mm in diameter and 100 μm thick. A thin aluminum film is then evaporated on the other side acting as an electrode and a piezoelectric disk 9 mm in diameter and 0.4 mm thick is glued to this side, constituting the bimorph transducer. The size of the microjet is about 14 mm × 14 mm and 1.2 mm thick and the whole drug delivery system is designed as a portable device with the total size of 18 mm in diameter and 120 mm long.

Driven by an electrical pulse with certain frequencies, the piezoelectric transducer generates a pressure wave, which propagates towards the nozzles in the fluid chamber and squeezes the liquid out. With enough kinetic energy the liquid releases through the nozzles and forms droplets. The piezoelectric microjet works at its resonant frequencies, and if vibrating in its higher mode, will obtain higher kinetic energy and flow rate. Therefore, it is necessary for the device to work at higher resonant frequencies to meet the application requirements, such as high flow rate, small droplet size and narrow size distribution. Fig. 3 indicates that a microjet with a nozzle diameter of 10 μm which is ejecting liquid droplets with the mean diameter of 15 μm driving by 40 V rectangular electrical signals with 79 kHz.

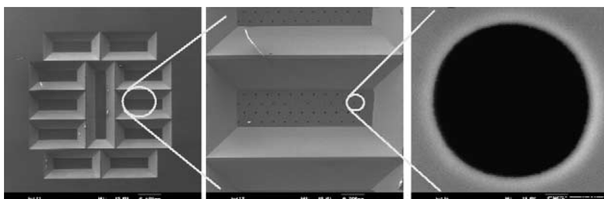

Fig. 2. SEM photos of the chip with nozzle arrays.

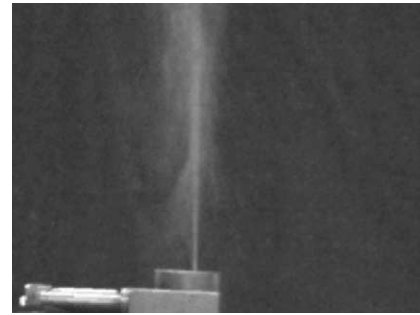

Fig. 3. A microjet in ejection of liquid droplets.

3. Different fields coupling analysis

3.1. Piezoelectricity–structure coupling model

In order to establish the piezoelectricity–structure coupling model for a bimorph transducer as illustrated in Fig. 4, the following conditions are assumed:

(1) the displacement of the transducer is small enough and all the materials are in their linear elastic range;
(2) each layer is continuous along the thickness direction, so the transverse deflection is the same along z-axis;
(3) there are no shear strains in the structure and only the flexural vibration is considered;
(4) the piezoelectric layer is polarized along z-direction and the thickness is thin enough so that the electric field is only along z-axis and keeps the same.

According to the above assumptions, the bending theory of thin plates is applicable. To further simplify the analysis, the structure is divided into two parts: one is a bimorph with the same diameter of $2b$ and the other is an annular plate with the diameter range from $2b$ to $2a$. The reference plane is located at the middle of the elastic plate. Therefore, the effective flexural rigidity of the piezoelectric disk D_1 is

$$D_1 = \frac{E_1}{1-\sigma_1^2}\int_{h_2}^{h_1+h_2} z^2\,dz = \frac{E_1 h_1^3}{3(1-\sigma_1^2)}\left(1+\frac{3}{2}\beta+\frac{3}{4}\beta^2\right) \quad (1)$$

where E_1 and σ_1 are the Young's modulus and the Poisson's ratio of the piezoelectric material, h_1 and $2h_2$ are the thicknesses of the piezoelectric disk and the elastic plate, respectively, and β is the thickness ratio of the elastic plate to piezoelectric disk. The effective flexural rigidity of the elas-

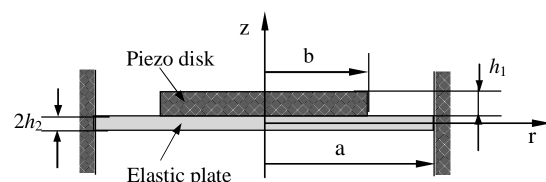

Fig. 4. Model of a silicon-piezoelectric bimorph transducer.

tic plate D_2 is

$$D_2 = \frac{E_2(2h_2)^3}{12(1-\sigma_2^2)} = \frac{2E_2h_2^3}{3(1-\sigma_2^2)} \quad (2)$$

where E_2 and σ_2 are the Young's modulus and the Poisson's ratio of the elastic material. Thus, the governing equation of the bimorph ($0 \leq r \leq b$) is

$$(D_1 + D_2)\nabla^4 w_1 + (\bar{m}_1 + \bar{m}_2)\frac{\partial^2 w_1}{\partial t^2} = 0 \quad (3)$$

where $\bar{m}_1$ and $\bar{m}_2$ are mass densities of the piezoelectric disk and the elastic plate per unit area, w_1 is the transverse deflection of the bimorph. Only considering axisymmetric vibration modes, the solution w_1 is assumed as

$$w_1 = W_1(r)\,\mathrm{e}^{\mathrm{j}\omega t} \quad (4)$$

where $W_1(r)$ is the shape function of the bimorph. Substituting Eq. (4) in Eq. (3), we get the differential equation of $W_1(r)$ as

$$(\nabla^2 + k_1^2)(\nabla^2 - k_1^2)W_1 = 0, \quad k_1^4 = \frac{\bar{m}_1 + \bar{m}_2}{D_1 + D_2}\omega^2 \quad (5)$$

In the same way, the governing equation of the annular plate ($b \leq r \leq a$) is given by

$$D_2\nabla^4 w_2 + \bar{m}_2\frac{\partial^2 w_2}{\partial t^2} = 0 \quad (6)$$

and the differential equation of $W_2(r)$ as

$$(\nabla^2 + k_2^2)(\nabla^2 - k_2^2)W_2 = 0, \quad k_2^4 = \frac{\bar{m}_2}{D_2}\omega^2 \quad (7)$$

where w_2 and $W_2(r)$ are the transverse deflection and shape function of the annular plate, respectively. Now the dynamic equations of the bimorph transducer have been obtained. To solve these equations, the following boundary conditions are assumed.

According to the assumption (4), stimulated by a harmonic electric voltage $v_z = V_0\,\mathrm{e}^{\mathrm{j}\omega t}$, an electric field along z-direction in the piezo disk is generated and the amplitude is given by

$$E_z = \frac{V_0}{h_1} \quad (8)$$

By the theory of piezoelectricity, a stress T_r^{P} is caused around the circumference and keeps the same along the thickness direction by

$$T_r^{\mathrm{P}} = -\frac{E_1 d_{31}}{1-\sigma_1}E_z = -\frac{E_1 d_{31} V_0}{(1-\sigma_1)h_1} \quad (9)$$

where d_{31} is the piezoelectric coupling coefficient. The stress is equivalent to a flexural moment M_v around the circumference $r = b$ as

$$M_v = \int_{h_2}^{h_1+h_2} T_r^{\mathrm{P}} z\,\mathrm{d}z = \int_{h_2}^{h_1+h_2} -\frac{E_1 d_{31} V_0}{(1-\sigma_1)h_1} z\,\mathrm{d}z = -\frac{E_1 h_1 d_{31} V_0}{2(1-\sigma_1)}(1+\beta) \quad (10)$$

and then, the continuous boundary conditions at $r = b$ are given by

$$W_1 = W_2, \quad \frac{\partial W_1}{\partial r} = \frac{\partial W_2}{\partial r}, \quad M_1 + M_v = M_2, \quad Q_1 = Q_2 \quad (11a)$$

where the flexural moments M_1 and M_2 are

$$M_1 = -\left\{D_1\left[\sigma_1\nabla^2 W_1 + (1-\sigma_1)\frac{\partial^2 W_1}{\partial r^2}\right] + D_2\left[\sigma_2\nabla^2 W_1 + (1-\sigma_2)\frac{\partial^2 W_1}{\partial r^2}\right]\right\},$$

$$M_2 = -D_2\left[\sigma_2\nabla^2 W_2 + (1-\sigma_2)\frac{\partial^2 W_2}{\partial r^2}\right]$$

and the transverse shearing forces are

$$Q_1 = -(D_1 + D_2)\frac{\partial\nabla^2 W_1}{\partial r}, \quad Q_2 = -D_2\frac{\partial\nabla^2 W_2}{\partial r}$$

Mechanical boundary conditions for the clamped edge ($r = a$) are

$$W_2 = 0, \quad \frac{\partial W_2}{\partial r} = 0 \quad (11b)$$

Combining Eqs. (5), (7) and (11a) and (11b), the dynamic model of the bimorph transducer is established. The general solutions of Eqs. (5) and (7) can be explained by Bessel functions

$$W_1 = A_1 J_0(k_1 r) + A_2 I_0(k_1 r) \quad (12a)$$

$$W_2 = A_3 J_0(k_2 r) + A_4 Y_0(k_2 r) + A_5 I_0(k_2 r) + A_6 K_0(k_2 r) \quad (12b)$$

where J_0 and Y_0 are the Bessel function of zero order of the first kind and the second kind, I_0 and K_0 are the modified Bessel function of zero order of the first kind and second kind, A_i ($i = 1, 2, \ldots, 6$) are constants depending on the boundary conditions. Substitute Eqs. (12a) and (12b) in Eqs. (11a) and (11b) and get

$$[H]\begin{bmatrix} A_1 \\ A_2 \\ A_3 \\ A_4 \\ A_5 \\ A_6 \end{bmatrix} = \begin{bmatrix} 0 \\ 0 \\ 0 \\ 0 \\ 0 \\ M_v \end{bmatrix} \quad (13)$$

where $[H]$ is a 6×6 matrix. By solving Eq. (13), A_i ($i = 1, 2, \ldots, 6$) can be got and then the mode shape functions of the transverse deflection are available. Utilizing the mode shape functions, we can obtain the solution under a harmonic electric voltage $v_z = V_0\,\mathrm{e}^{\mathrm{j}\omega t}$.

When using a rectangular electric voltage, this can be factorized into a series of harmonic electric voltages. Thus, the equations can be solved for each harmonic signal and the

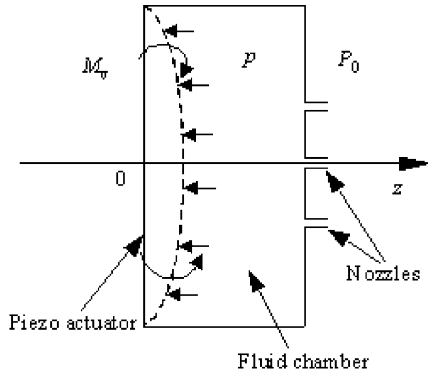

Fig. 5. Cross-section schematic of a piezoelectric microjet.

overall system response is achieved by adding up all these solutions, that is the displacement response of the transducer for this mode. However, it is very difficult to solve the equations directly. Therefore, a numerical simulation method has been used in the later part of this paper.

3.2. Fluid–structure coupling analysis

The piezo–structure coupling model of the transducer has been established as the above. When the device is in action, the liquid will be pushed out of nozzles by the flexural vibration, generating a reverse reaction on the transducer. The structural vibration and the microfluidic flow are also coupled. Fig. 5 shows the cross-section schematic of the microjet, taking into account this coupling.

Here the actuator has the same structure as the transducer mentioned above and is considered during the period of contraction and ejection of droplets. Due to the small dimension of the fluid chamber, the pressure is assumed the same in the whole fluid chamber. Although the fluid–structure coupling has some effects on the resonant frequencies and vibration amplitude of the device, the impact on the mode shapes of the bimorph transducer is negligible [8].

Thus, considering the fluid-coupling effect, the dynamic equations of the transducer are modified as following:

$$(D_1 + D_2)\nabla^4 w_1 + (\bar{m}_1 + \bar{m}_2)\frac{\partial^2 w_1}{\partial t^2} = -\Delta p, \quad 0 \le r \le b \tag{14a}$$

$$D_2\nabla^4 w_2 + \bar{m}_2\frac{\partial^2 w_2}{\partial t^2} = -\Delta p, \qquad b \le r \le a \tag{14b}$$

where Δp, the pressure difference between the fluid chamber and the air, is given by

$$\Delta p = C_{DS}\frac{\rho_w}{2A^2}Q^2 + \frac{4\sigma_w}{d} \tag{15}$$

where C_{DS} is the total loss coefficient of pressure, ρ_w and σ_w are the density and surface tension of the working liquid, d the diameter of the nozzles, A the area of the transducer and Q the rate of the liquid. When the diameter of nozzles is very small, viscosity and surface tension are the main forces the device should overcome. According to the solid mechanics, the pressure difference Δp should be known before solving Eqs. (14a) and (14b). On the other hand, only after solving the Navier–Stokes equation, Δp can be obtained. However, to solve the Navier–Stokes equation, the velocity of the transducer surface has to be known, which makes it necessary to solve Eqs. (14a) and (14b) and the Navier–Stokes equation simultaneously, while the tremendous calculation work makes it impossible. Therefore, an approximate model is provided here to give the relationship between the pressure difference and the velocity of the transducer surface, uncoupling the equation and solving it separately.

Volume change of the fluid chamber V is given as

$$V = \int_0^b w_1\, 2\pi r\, dr + \int_b^a w_2\, 2\pi r\, dr \tag{16}$$

According to the fluid continuous equation and the geometric characteristics of fluid chamber, the relationship between the fluid rate and the volume change of the chamber is described by

$$Q = \dot{V} \tag{17}$$

Combining Eqs. (14a), (14b), (15) and (17), the uncoupled dynamic equations are given by

$$(D_1 + D_2)\nabla^4 w_1 + C_{DS}\frac{\rho_w}{2A^2}\dot{V}^2 + (\bar{m}_1 + \bar{m}_2)\frac{\partial^2 w_1}{\partial t^2} = -\frac{4\sigma_w}{d}, \qquad 0 \le r \le b \tag{18a}$$

$$D_2\nabla^4 w_2 + C_{DS}\frac{\rho_w}{2A^2}\dot{V}^2 + \bar{m}_2\frac{\partial^2 w_2}{\partial t^2} = -\frac{4\sigma_w}{d}, \quad b \le r \le a \tag{18b}$$

All boundary conditions are the same as the above. Because Eqs. (18a) and (18b) is a non-linear equation, it is quite difficult to obtain analytical solutions. In the next part, by finite-element method, the fluid–structure coupling situation is simulated.

4. Simulation of coupling interactions

The theoretical models for the transducer under piezoelectricity–structure coupling and fluid–structure coupling have been established above in this paper, which illustrates the working mechanism of the device under loading conditions. However, owing to the complexity of the models, the analytical solutions are formidable to obtain. The finite-element method [9] is very suitable to solve this problem since it can be applied to any geometry and for any set of materials' properties and loading conditions as long as the appropriate constitutive relationships and equilibrium conditions are met. In our work, ANSYS was used to calculate the dynamic responses of the device under water-loading

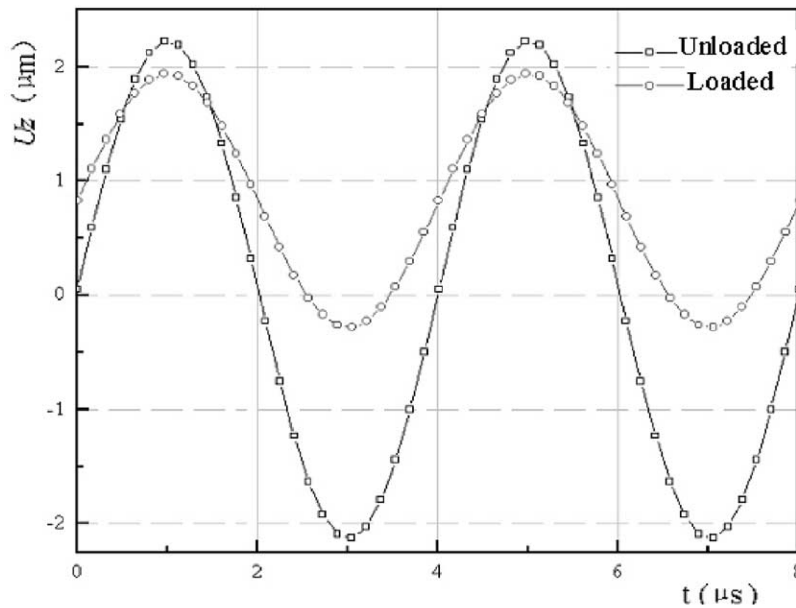

Fig. 6. Dynamic displacement of the transducer center.

conditions, demonstrating the coupling effects on the performance of the device.

Since the device structure is symmetric, a finite-element model using only one-quarter of the structure is possible. The size of the two silicon chips is 14 mm × 14 mm × 0.4 mm with the clamped boundaries and the elastic chamber membrane is Ø10 mm × 0.1 mm and the piezoelectric disk Ø10 mm × 0.4 mm.

When the device is in action, the liquid will induce a counterforce on the transducer and thus impact on the characteristics of the microjet. The device is driven by a rectangular-shape signal with a direct current (dc) offset, which can be divided into two parts, a dc signal and a rectangular alternating current (ac) signal with the same frequency.

From experimental results, when the device is working steadily, the frequency of the response has the same frequency of the controlling signal, which indicates that the fluid–structure coupling has little effects on the resonant frequencies. In this case, the coupling can be considered as a force load with the same frequency and the inverse phase to the driving electric signal. In the same way, the force can be divided into two parts as a static force load and a dynamic force load. Calculating the static response of the device under the dc electric signal, the static force load and the dynamic response under the ac electric signal, and the dynamic force load, respectively, the total response of the device can be obtained by combining the static and the dynamic responses.

Assuming that the device vibrates in a higher resonant mode, at $f = 250\,\mathrm{kHz}$, with the diameter of the nozzles of 5 μm, a voltage amplitude of the driving signal of 40 V, and according to Eq. (15), the amplitude of the pressure difference about 0.1 MPa, the characteristics of the device are thoroughly simulated and compared. From the simulation results, the dynamic displacements of the transducer center under liquid-loading and unloading are extracted as shown in Fig. 6.

The comparison of the transducer displacements illustrates that the basic shapes of the displacements under the loading and unloading conditions are almost the same while the amplitude of the displacements under loading decreases significantly. From the simulation results, the peak-to-peak value of the displacement under the loading condition is about one-half of that under the unloading condition.

Based on the simulation results for the coupling interactions of different physical effects, although the fluid–structure coupling can dramatically damp the vibration amplitude, it has little impacts on the resonant frequencies of the device. Thus, during further optimum design, the structure of the device, the coupling effects are assumed negligible to decrease the calculation work. Based on the maximum volume change of the fluidic chamber, the device has been optimized and fabricated.

5. Conclusions

In this paper, we have fabricated a piezoelectrically actuated microjet, studied the working mechanism of the device and established the coupling models of the device by simplifying the coupling interactions. The non-linear coupling models are formidable to solve. Thus, by finite-element method, the characteristics of the device are thoroughly studied, and the dynamic responses of the transducer under liquid-loading and unloading conditions are compared. Just as the experimental results indicated, the simulation results show that the coupling interactions can dramatically damp

the vibration amplitude of the transducer, but has little impact on the resonant frequencies. Therefore, during optimum design of the device structure, neglecting the coupling effects becomes sound and can save tremendous calculation work.

Acknowledgements

Financial support by National Natural Science Funds (29833070) and National 973 Basic Research Projects (G1999033106) of China is deeply appreciated.

References

[1] K.W. Stapleton, W.H. Finlay, Determining solution concentration within aerosol droplets output by jet nebulizers, J. Aerosol Sci. 26 (1) (1995) 137–145.
[2] G. Percin, L. Levin, B.T. Khuri-Yakub, Piezoelectrically actuated transducer and droplet ejector, in: Proceedings of the IEEE Ultrasonics Symposium, 1996, pp. 913–916.
[3] Ph. Luginbuhl, P. Indermuhle, M. Gretillat, Micromachined injector for DNA mass spectrometry, in: Proceedings of the Transducers'99, Sendai, Japan, 1999, pp. 1130–1133.
[4] K. Tang, A. Gomez, Generation by electrospray of monodisperse water droplets for targeted drug delivery by inhalation, J. Aerosol Sci. 25 (6) (1994) 1237–1249.
[5] B. de Heij, B. van der Schoot, H. Bo, J. Hess, N.F. de Rooij, Characterisation of a fL droplet generator for inhalation drug therapy, Sens. Actuators A 85 (3) (2000) 430–434.
[6] C. Liu, Z. Zhou, X. Wang, J. Xiong, A piezoelectrically actuated microjet, in: Proceedings of the Fourth International Symposium on Test and Measurement, Shanghai, China, 2001.
[7] B. de Heij, B. van der Schoot, N.F. de Rooij, H. Bo, J. Hess, Modelling and optimization of a vaporizer for inhalation drug therapy, in: Proceedings of the Second International Conference on Modelling and Simulation of Microsystems, 1999, pp. 542–545.
[8] M.K. Kwak, K.C. Kim, Axisymmetric vibration of circular plates in contact with fluid, J. Sound Vib. 146 (3) (1991) 381–389.
[9] W. Hwang, H.C. Park, Finite-element modeling of piezoelectric sensors and actuators, AIAA J. 30 (3) (1992) 930–937.

Biographies

Changgeng Liu received a PhD degree from Tsinghua University, China, in 2001. He joined Center for Advanced Microstructures and Devices, Louisiana State University, as a Postdoctoral Research Associate in 2002. He has been working in the fields of MEMS since 1996. His current research activities include micromachining, Microfluidics, MEMS and BioMEMS.

Tianhong Cui is serving as the Nelson Associate Professor of Mechanical Engineering at University of Minnesota. He received the BS from Nanjing University of Aeronautics and Astronautics in 1991, and PhD from Chinese Academy of Sciences in 1995. He has 10 years of experience in the field of MEMS. He has conducted research and development work for the realization of microsensors, microactuators, and microsystems since 1991. Prior to joining the Institute for Micromanufacturing as an assistant professor in 1999, he was at the National Laboratory of Metrology in Japan (a premier microsystems development center) as a Research Fellow, and previous to that, served as a Postdoctoral Research Associate in Dr. Dennis Polla's MEMS group at the University of Minnesota. His current research interests include polymer micro/nanoelectronics, MEMS, and nanotechnology.

Zhaoying Zhou graduated from the Department of Precision Instruments, Tsinghua University, Beijing, China, in 1961. He is the academic chairman of the Micro-Nano Technology Research Center, Tsinghua University. He is also a council member of Chinese Instrument Society, Vice-president of China Instrument Society, Deputy Chief Editor of the Journal of the Chinese Instrumentation. His present research interests focus on the measurement, control and microelectromechanical systems.

Kun Lian is an Assistant Professor at Center of Advanced Microstructures and Devices (CAMD) at Louisiana State University, Louisiana. He received his BS in chemical engineering at the South China University of Technology, and MS and PhD degrees in engineering science (Material Science) from Louisiana State University in 1991 and 1995, respectively. His research interests include material characterization, thin film sensors, environmental induced material property changes, testing of material property modifications of MEMS materials.

Jost Goettert is the Director for Microfabrication in CAMD at Louisiana State University. He received a Master Degree in physics from the University of Bonn, Germany, in 1987, and graduated in mechanical engineering from the University of Karlsruhe in 1992. He worked as a Post-Doc with the Institut fuer Mikrostrukturtechnik at Forschungszentrum Karlsruhe until 1996, a Research Engineer in the Institute for Micromanufacturing at LaTech University in Ruston, Louisiana (1996 and 1997) and a Scientific Staff Member at the ANKA synchrotron facility at Forschungszentrum Karlsruhe (1998 and 1999). Since 2000 he is the Director for Microfabrication at CAMD focusing on building and establishing a LIGA service for the MEMS community. Current fields of interest include X-ray microfabrication, applications of LIGA in the field of BioMEMS, and developing of molding processes of high aspect ratio microstructures using novel materials.